Journal of Applied Physics

Metal-functionalized 2D boron sulfide monolayer material enhancing hydrogen storage capacities

Cite as: J. Appl. Phys. **127**, 184305 (2020); https://doi.org/10.1063/5.0008980
Submitted: 30 March 2020 . Accepted: 25 April 2020 . Published Online: 12 May 2020

Pushkar Mishra, Deobrat Singh, Yogesh Sonvane, and Rajeev Ahuja

Journal of Applied Physics ARTICLE scitation.org/journal/jap

Metal-functionalized 2D boron sulfide monolayer material enhancing hydrogen storage capacities

Cite as: J. Appl. Phys. **127**, 184305 (2020); doi: 10.1063/5.0008980
Submitted: 30 March 2020 · Accepted: 25 April 2020 ·
Published Online: 12 May 2020

Pushkar Mishra,[1] Deobrat Singh,[2,a)] Yogesh Sonvane,[1,a)] and Rajeev Ahuja[2,3,a)]

AFFILIATIONS

[1]Applied Material Lab, Department of Applied Physics, S. V. National Institute of Technology, Surat 395007, India
[2]Condensed Matter Theory Group, Department of Physics and Astronomy, Uppsala University, Box 516, 75120 Uppsala, Sweden
[3]Applied Materials Physics, Department of Materials and Engineering, Royal Institute of Technology (KTH), S-100 44 Stockholm, Sweden

[a)]**Authors to whom correspondence should be addressed:** yas@phy.svnit.ac.in; deobrat.singh@physics.uu.se; and rajeev.ahuja@physics.uu.se

ABSTRACT

In the present work, we have systematically investigated the structural, electronic, vibrational, and H_2 storage properties of a layered 2H boron sulfide (2H-BS) monolayer using spin-polarized density functional theory (DFT). The pristine BS monolayer shows semiconducting behavior with an indirect bandgap of 2.83 eV. Spin-polarized DFT with van der Waals correction suggests that the pristine BS monolayer has weak binding strength with H_2 molecules, but the binding energy can be significantly improved by alkali metal functionalization. A system energy study indicates the strong bonding of alkali metals with the BS monolayer. The Bader charge analysis also concludes that a considerable charge is transferred from the metal to the BS monolayer surface, which was further confirmed by the iso-surface charge density profile. All functionalized alkali metals form cations that can bond multiple H_2 molecules with sufficient binding energies, which are excellent for H_2 storage applications. An ideal range of adsorption energy and practicable desorption temperature promises the ability of the alkali metal functionalized BS monolayer as an efficient material for hydrogen storage.

I. INTRODUCTION

There are two major concerns across the world: one is the annihilation of non-renewable energy sources, and the other is climate change because of environmental pollution. Out of many available solutions, hydrogen (H_2) is outstanding due to having the highest energy density, high availability, and eco-friendliness, hence having the ability to become effective energy carriers.[1–4] However, some challenges such as storage, production, and transport limit the use of hydrogen as a clean renewable energy source. Out of all of these challenges, the toughest challenge is the too large scale storage of hydrogen within ambient conditions. The proposed target for H_2 storage by the US Department of Energy (DOE) is specified with a system gravimetric capacity range of 4.5%–6.5%, system volumetric capacity of 30 g/l, operating ambient temperature of 233 K–333 K, min/max delivery temperature of 233 K–358 K, and max delivery from storage system of 12 bar for onboard vehicle applications.[5,6] There are two main requirements for hydrogen storage: one is that the binding energy of hydrogen between chemisorption and physisorption should be within the 0.1–0.2 eV/H_2 range,[7] and another requirement is the selection of a storage material of lighter elements. However, it is difficult to fulfill these two criteria at the same time, since hydrogen is bonded either too strongly with light elements, forming metal hydrides, or too weakly with BN fullerenes and other heavier elements.[8]

The emergence of 2D materials led to a new phase in materials science due to their exclusive physical and chemical properties.[9,10] A number of recent studies have shown that 2D materials can store H_2 in a huge amount.[1,3,11–17] Boron based 2D materials such as boron nitride (BN) and borophene were supposed to be potential hydrogen storage materials because of their high surface to volume ratio, porous design, and particularly light weight. But pristine boron nitride and borophene have much less binding energy between H_2 and the sheet; for boron nitride, it is 0.05 eV/H_2 for

$6H_2$ molecules, and for borophene, it is 0.045 eV/H_2 for adsorption of one H_2.[18,19] This difficulty has been solved by intermediate adsorption of light transition metals (TMs), alkali metals (AMs), alkaline metals (ALMs), and non-metals (NMs) between the sheet and hydrogen molecules that enhance the ultimate binding energy and efficiency of hydrogen storage.[18–25] Here, we have chosen alkali metals (AMs) such as Li, Na, and K for intermediate adsorption, as there are a lot of significant factors for them and one of the most important factors is that their binding energy ratio to corresponding cohesive energies is much higher than that of heavier elements such as Sc and Ti transition metals. This would minimize the chances of cluster formation. Another important factor is that they are light weighted (less atomic masses), which makes the storage material lighter and the weight % of hydrogen increases. The mechanism of the interaction of hydrogen molecules with these metal ions (Li^+, Na^+, and K^+) justifies the advantage of taking Li, Na, and K for high hydrogen storage capacity. According to Niu *et al.*[26] when metal cations like Li^+, Na^+, and K^+ interact with hydrogen molecules, charge polarization induces and the hydrogen molecules become stretched and ultimately hydrogen coverage increases, which makes desorption also easier. According to Kubas's mechanism,[27] transition metals such as Sc, Ti, Pd, and Pt interact with an H_2 molecule, which gives an electron to the vacant d orbital of a transition metal and the transition metal also transfers back an electron to the H_2 molecule. Hence, the bonding can be defined based on the hybridization of the d orbital of the metal with the s orbital of hydrogen. Also, the main difficulty of transition metal functionalization is that they tend to cluster on the material's monolayer. Apart from all these, there is another reason to avoid the use of transition metals: they have high atomic mass, which reduces gravimetric density (weight %).

Recently, a new layered monochalcogenide, boron sulfide (BS) has been investigated by density functional theory (DFT), which comprises two hexagonal layers of BS that is bonded with boron–boron atoms. The calculated phonon dispersion curve that has no imaginary frequency confirms the dynamic stability of the layered material. Its mechanical properties such as higher tensile strength and stretchability make it strong and support novel applications. The ultimate tensile strength across the zigzag path was obtained as 0.26,[28] which is comparable to that of graphene (0.27)[29] and hexagonal boron nitride (0.30).[30]

Encouraged by these fascinating features of the BS monolayer, we have investigated structural, electronic, and vibrational properties and also explored the tendency to H_2 adsorption with a pristine sheet. But the adsorption energy of hydrogen with a pristine sheet is very less; therefore, we functionalized the sheet with alkali metals such as Li, Na, and K and investigated the electronic properties, charge transfer mechanism of hydrogenation, and dehydrogenation process of the BS monolayer.

II. COMPUTATIONAL METHODOLOGY

We employed spin-polarized density functional theory (DFT) to investigate the structural and electronic properties and H_2 storage characteristics of the pristine and alkali metal furnished BS monolayer by using the Vienna *ab initio* Simulation Package (VASP)[31,32] software. Exchange correlation interactions were approached by generalized gradient approximation (GGA) with the PBE method defined by Perdew *et al.*[33,34] We utilized the van der Waals correction of the DFT-D2 method introduced by Grimme[35] to escape the undervaluation of binding energy produced by the GGA method. The kinetic energy cutoff was taken as 500 eV in this calculation. The convergence criteria for force and energy were chosen as 0.001 eV/Å and 10^{-6} eV, respectively. For a sampling of the Brillouin zone, k-points were taken as $5 \times 5 \times 1$ for both the relaxation and density of states (DOS) following the Monkhorst–Pack scheme.[36] A vacuum of 15 Å was introduced to prevent the possible effects of the layers in a vertical direction. The binding energies of alkali metals (AMs), (E_b^{AM}), with the BS sheet were calculated by using the following equation:

$$E_b^{AM} = E_{AM+BS} - E_{BS} - E_{AM}, \quad (1)$$

where E_{AM+BS}, E_{AM}, and E_{BS} are the total energies of the BS sheet functionalized with alkali metals (AMs) Li, Na, and K, the total energy of AM elements, and the total energy of pristine BS sheet, respectively. The adsorption energy per H_2 molecule is determined by the following equation:

$$E_{ad} = \frac{E_{BS+AM+nH_2} - E_{BS+AM} - nE_{H_2}}{n}, \quad (2)$$

where $E_{BS+AM+nH_2}$ is the total energy of the hydrogen adsorbed metal functionalized BS sheet, E_{BS+AM} is the total energy of the metal functionalized BS sheet, E_{H_2} is the energy of hydrogen molecules, and n indicates the number of hydrogen molecules. We have also performed the Bader charge analysis for a better understanding

TABLE I. Calculated lattice parameter, bond angle, and bond length of the BS monolayer.

Lattice parameter (Å)	Bond angle (deg)	Bond length (Å)
a = 3.041	∠BSB = 102.426	B–B = 1.95
b = 3.041	∠SBS = 102.426	B–S = 1.78
	∠SBS = 115.835	S–S = 3.43

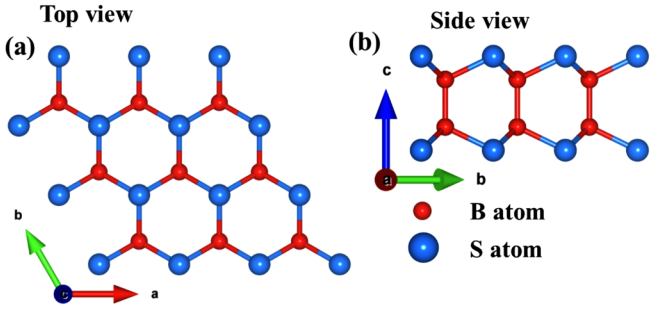

FIG. 1. (a) Top and (b) side views of the pristine 2H-BS monolayer.

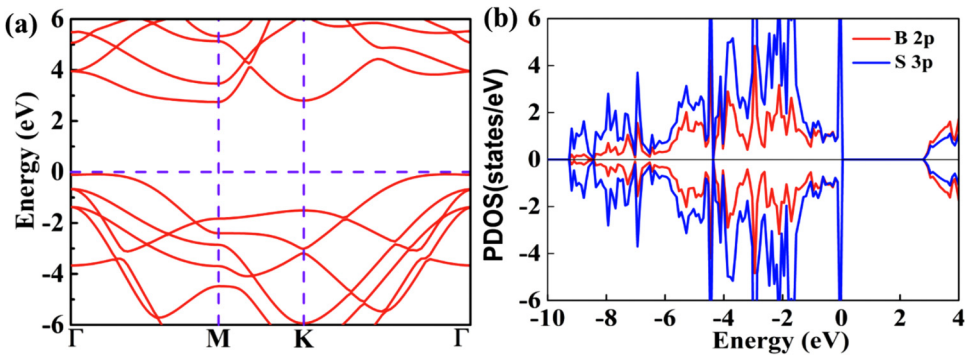

FIG. 2. (a) Band structure and (b) spin-polarized partial density of states of boron (B-2p) and sulfur (S-3p) atoms in the pristine BS monolayer.

of the charge transfer mechanism between the BS sheet and alkali metals like Li, Na, and K.

III. RESULTS AND DISCUSSION

A. Structural, electronic, and vibrational properties of the pristine BS monolayer

First, we examined the structural properties of the BS monolayer to check the efficiency of the computational methodology used in this work. The structural properties such as lattice parameter, bond angle, and bond length are described in Table I. We found that our calculated results are in excellent agreement with an earlier study.[28,37] The top and side views of BS are shown in Fig. 1.

To examine the electronic properties of the BS monolayer, we plotted the band structure and spin-polarized partial density of states (PDOS). Figure 2(a) presents the band structure and Fig. 2(b) shows the PDOS plot of the BS monolayer. We measured the bandgap using the PBE functional which is 2.83 eV, almost the same as previously reported.[28] From the band structure, we observe that the valance band maxima (VBM) exist near the Γ point and the conduction band minima occur near the M point. The band structure indicates that the BS monolayer is an indirect, wide bandgap semiconductor. From Fig. 2(b), the PDOS plot also conveys the wide bandgap in the valance band in which the major contribution near the Fermi level originates from the S (3p) orbitals.

To investigate the dynamic stability of the BS monolayer, we have calculated the phonon dispersion curve, which is shown in Fig. 3. As it is noticeable from Fig. 3(a), there is no imaginary frequency in phonon dispersion, indicating the dynamic stability of the BS monolayer. For further understanding of the phonon spectrum, we have also calculated the vibrational density of states (VDOS), as shown in Fig. 3(b). From Fig. 3(b), we illustrated that, in the acoustic branch, the S atom dominates over the boron atom and a highest peak at 1.53 states/THz was obtained around the 11.22 THz frequency. However, in the optical branch due to the lighter mass, B dominantly contributes to the VDOS spectra. Two gaps are obtained in frequency, the first is around 12.9 THz–17.7 Thz and the second is around 23.10 THz–27.60 THz.

B. Hydrogenation of the pristine BS monolayer

At first, we studied the sensory interaction of the H_2 molecule with a pristine BS monolayer. In this analysis, we put the H_2 molecule at nearly 1.5 Å above the monolayer. We have calculated the adsorption energy of the H_2 molecules with the monolayer. The calculated value of adsorption is given in Table II, as illustrated in Fig. 4, which shows that the interaction of the H_2 molecule with the

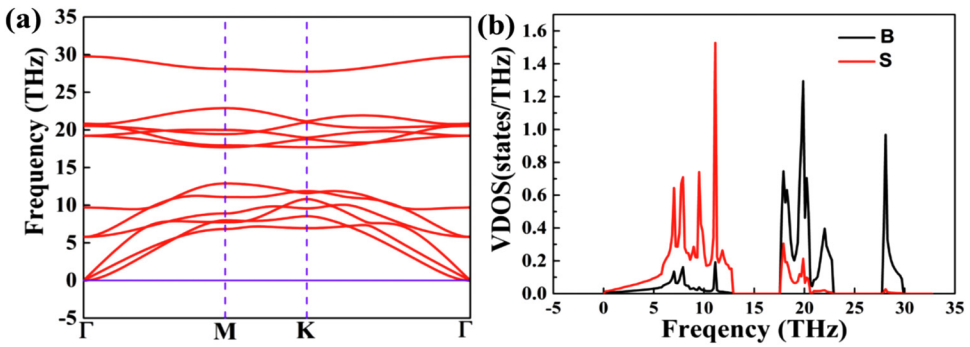

FIG. 3. (a) Phonon dispersion curve and (b) vibrational density of states (VDOS) of the BS monolayer.

TABLE II. Calculated adsorption energy and charge transfer of H_2 molecule with the pristine BS sheet.

System	Adsorption energy per H_2 (eV)	Charge transfer from sheet to per H_2 molecule
$1H_2$@BS	−0.0393	0.00633
$2H_2$@BS	−0.0419	0.00562
$3H_2$@BS	−0.0448	0.00483
$4H_2$@BS	−0.0445	0.00454

TABLE III. The binding energy (E_b) of alkali metals to the BS sheet, Q_a charge on the alkali metal atom before adsorption, and Q_b charge on the alkali metal atom after adsorption. ΔQ is the charge transfer to the BS sheet from the alkali metal atom.

System	E_b^{AM}(eV)	Q_a (a.u.)	Q_b (a.u.)	(ΔQ) (a.u.)
Li@BS	−4.48	1.000 000	0.007 631	0.9924
Na@BS	−4.05	1.000 000	0.230 990	0.7690
K@BS	−5.52	9.000 000	8.219 558	0.7804

pristine BS monolayer is very poor. Therefore, we cannot use a pristine BS monolayer for further H_2 storage applications in ambient conditions. For adsorption energy calculations, we used the formula

$$E_{ads} = \frac{E_{BS+nH_2} - E_{BS} - nE_{H_2}}{n}, \quad (3)$$

where E_{BS+nH_2}, E_{BS}, and E_{H_2} denote the total energy of a complex system (hydrogenation of the BS monolayer), the energy of the BS monolayer, and the energy of isolated H_2 molecules. Here, n is the number of hydrogen molecules present on the surface of the BS monolayer.

C. Functionalization of BS with alkali metals (Li, Na, and K)

To improve the adsorption energy of the H_2 molecules, we first functionalized the monolayer with alkali metals (Li, Na, and K), and then functionalized the BS sheet that would be utilized for hydrogen storage. For achieving the lowest energy configuration, we placed a single atom of alkali metals on all possible adsorption positions over the BS sheet including the top of the S atom, B atom, bridge of the B–S, and hallow site (four positions). Based on energy optimization among all four positions, the bridge of the B–S position is the most suitable position. Now, these optimized structures and the BS sheet functionalized with one alkali metal were used for hydrogen storage. All the optimized structures are shown in Fig. 5.

The calculated binding energies (E_b^{AM}) for single metal dopant adatoms Li, Na, and K above the bridge of the B–S position are −4.48 eV, −4.05 eV, −5.52 eV, respectively, which is represented in Table III. These binding energies (E_b^{AM}) are sufficiently high compared to their corresponding cohesive energies (E_c) −1.63 eV (Li), −1.11eV (Na), and −0.93eV (K).[38] This makes it clear that the alkali metals Li, Na, and K are uniformly distributed over the BS sheet without being clustered.

To investigate the electronic properties of the alkali metal functionalized BS monolayer, we sketched the spin-polarized partial density of states (PDOS). Figures 6(a)–6(c) represent the PDOS plot of Li@BS, Na@BS, and K@BS, respectively. As in pure BS, there is a wide bandgap of 2.83 eV; when we placed alkali metal atoms such as Li, Na, and K, this gap will be shifted from the conduction band to the valance band. As shown in Fig. 6(a) in the case of Li, due to the low ionization energy, Li's 2s valance electron was donated to the BS sheet to fill the vacant conduction band, because the charge transfer (~0.99 |e| from the Bader charge analysis) on the bottom of the conduction band moves toward the Fermi

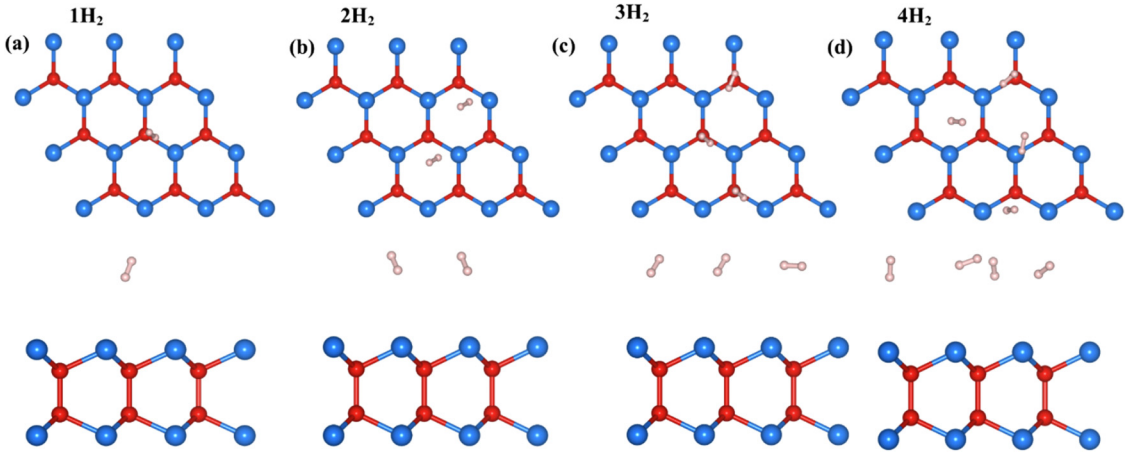

FIG. 4. Top and side views of hydrogenation of a pure BS monolayer for (a) $1H_2$, (b) $2H_2$, (c) $3H_2$, and (d) $4H_2$.

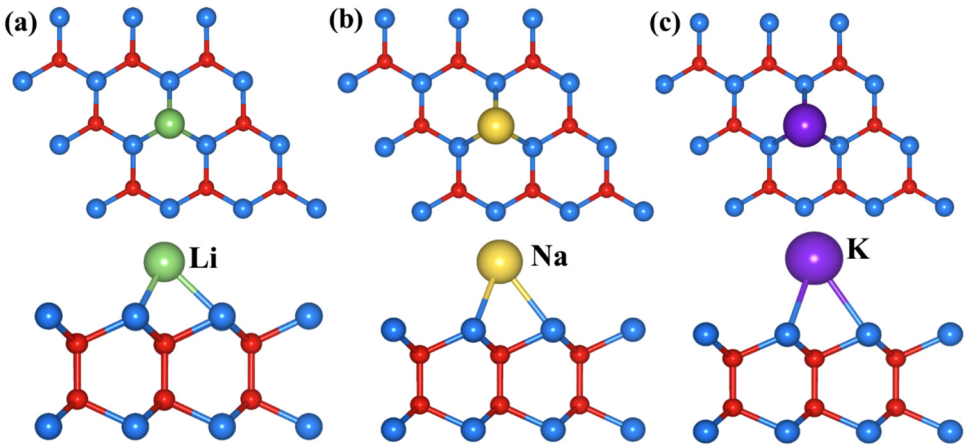

FIG. 5. Top and side views of alkali metals (a) Li, (b) Na, and (c) K functionalized BS monolayer.

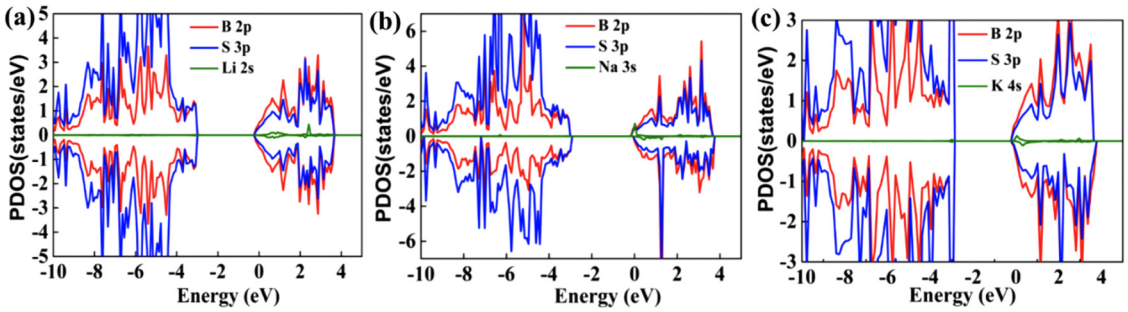

FIG. 6. Projected density of states of the alkali metal functionalized BS sheet: (a) Li@BS, (b) Na@BS and (c) K@BS.

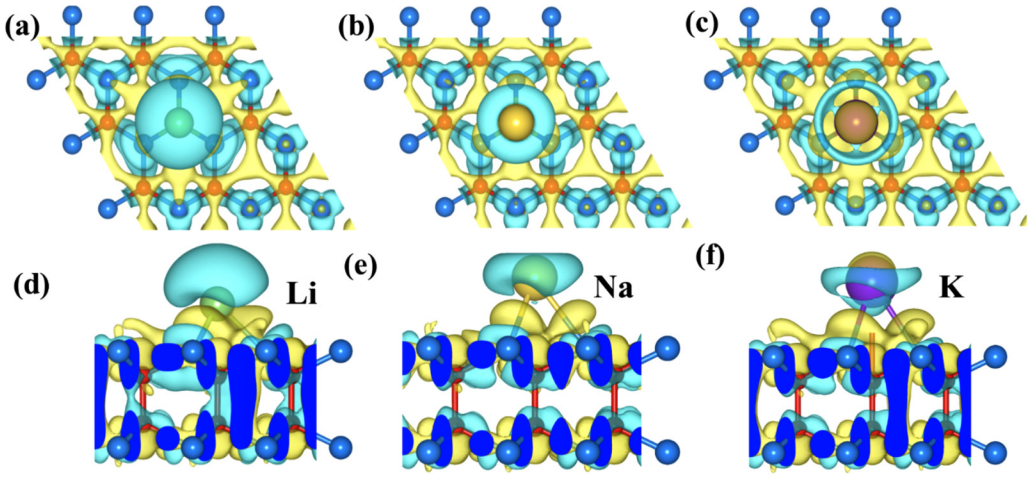

FIG. 7. (a)–(c) Top views and (d)–(f) side views of isosurface charge density plots with an isovalue of 0.001 eV/Å^3 of the alkali metals (Li, Na, and K) functionalized BS sheets, respectively. Yellow and cyan show the accumulation and depletion of charges, respectively.

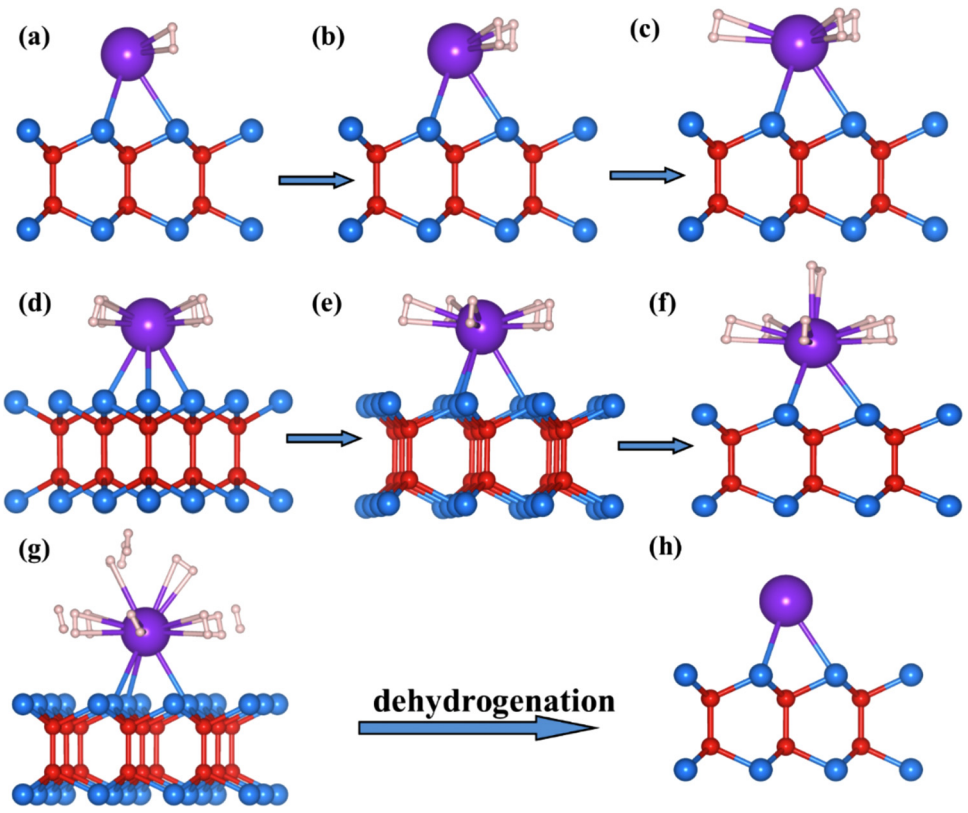

FIG. 8. (a)–(h) represent the hydrogenation for $1H_2$, $2H_2$, $3H_2$, $4H_2$, $5H_2$, $6H_2$, and $12H_2$ and dehydrogenation process of the K functionalized BS monolayer, respectively.

level (0.0 eV). The PDOS of Na and K with the BS sheet shows the same characteristic to that of Li and are shown in Figs. 6(b) and 6(c). These results revealed that the bonding between the alkali metal atom and the BS sheet is mainly ionic. This is also confirmed by the Bader charge analysis.

1. Bader charge analysis

The charge transfer to the BS sheet from the alkali metals is determined by using the following equation:

$$\Delta Q = Q_a - Q_b, \tag{4}$$

where ΔQ is a difference in the Bader charge and Q_a and Q_b ascribe the atomic Bader charges before and after adsorption of alkali metals, respectively. They showed that a considerable amount of charge shifted from the alkali metals to the BS sheet.

We have plotted iso-surface charge density plots as shown in Fig. 7. We observed that the charge donated by the alkali metals mostly accumulated on the nearest sulfur atoms of the sheet, and a small part is gained by the boron atom. We also noticed that the Li atom transferred the maximum charge and the Na and K atoms transferred nearly equal charges that are also recommended by the Bader charge analysis.

D. Hydrogenation and dehydrogenation of the functionalized BS monolayer

In this segment, we will explain the adsorption and de-adsorption processes of H_2, with the alkali metals (Li, Na, and K) functionalizing the BS sheet. As can be observed from the Bader charge analysis and study of the partial density of states (PDOS), a large amount of charge transferred from the alkali metals to the BS sheet; as a result, a strong ionic bond formed between them, and the alkali metals were left in the cationic states. Consequently, partly positive alkali metals (Li^+, Na^+, and K^+) serve as a binding site for inserted H_2 molecules. At first, we inserted a single H_2 molecule in each alkali metal (Li, Na, and K) and enabled the system to achieve a ground state configuration via full structure optimization. By attempting multiple initial structures, it is observed that the vertical access of H_2 molecules to the alkali metals is favorable. The inserted H_2 molecules become polarized when engaging cationic alkali metal atoms and bound with them via electrostatic and van der Walls interactions.

To improve the storage capacity of H_2, we inserted more H_2 molecules in the alkali metal functionalized BS sheet by a systematic approach as shown in Figs. 8–10. In the second step, we inserted two H_2 molecules and enabled the systems again to go through full structure optimization. Similarly, we inserted three, four, five, and six H_2 molecules in the alkali

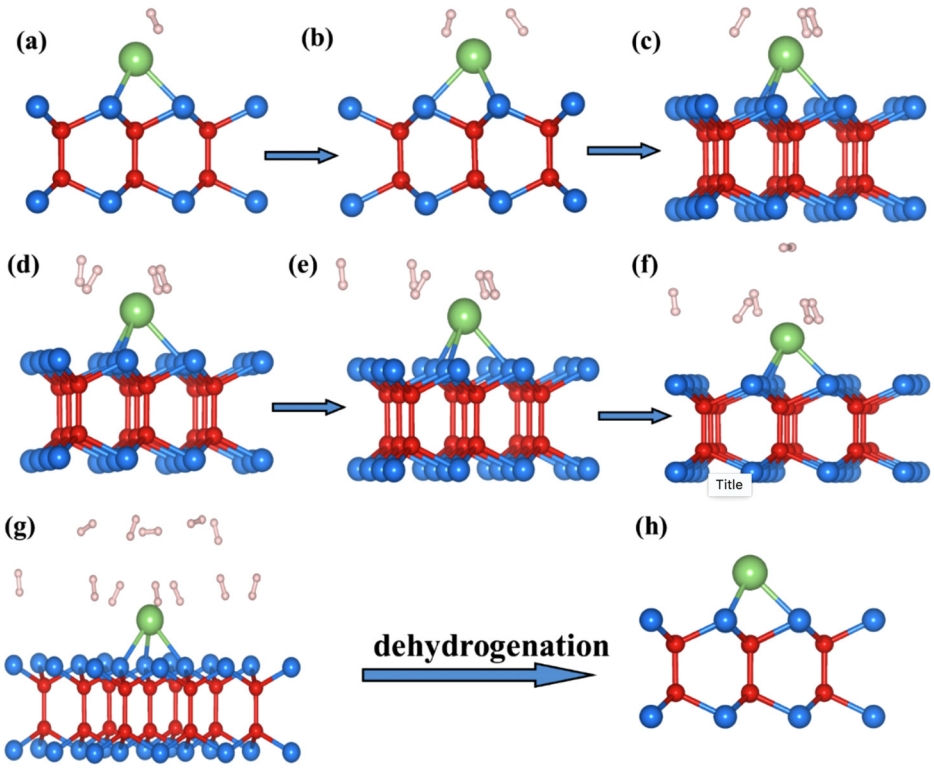

FIG. 9. (a)–(h) represent the hydrogenation for $1H_2$, $2H_2$, $3H_2$, $4H_2$, $5H_2$, $6H_2$, and $12H_2$ and dehydrogenation process of the Li functionalized BS monolayer, respectively.

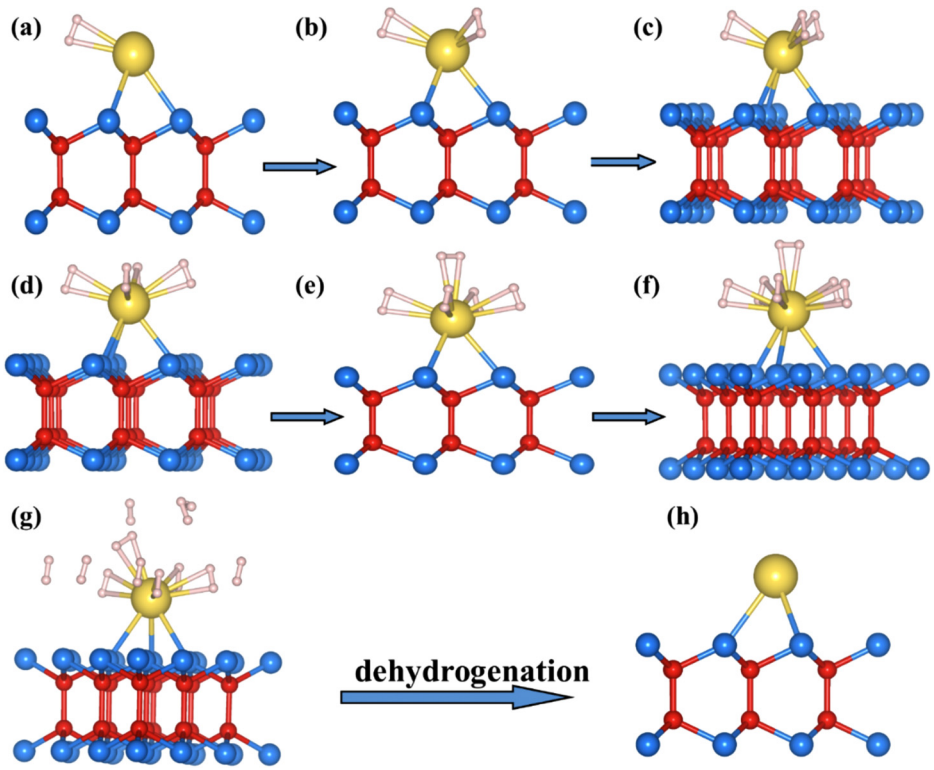

FIG. 10. (a)–(h) represent the hydrogenation for $1H_2$, $2H_2$, $3H_2$, $4H_2$, $5H_2$, $6H_2$, and $12H_2$ and dehydrogenation process of the Na functionalized BS monolayer, respectively.

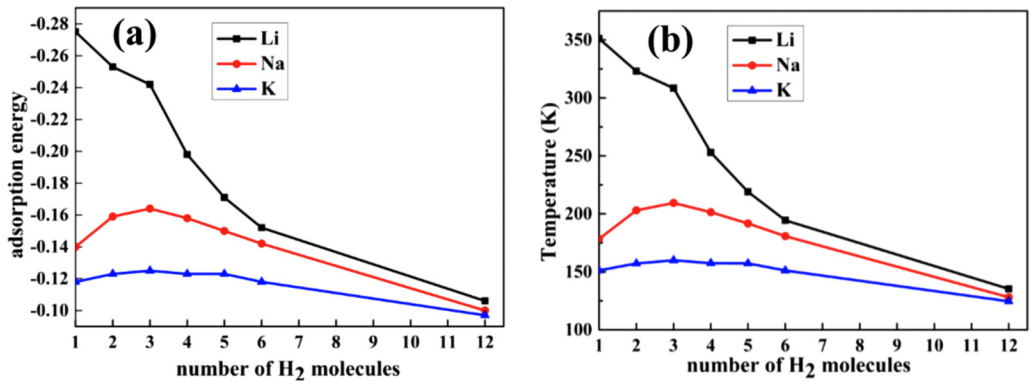

FIG. 11. (a) The variation of adsorption energy and (b) the corresponding desorption temperature as a function of H_2 molecules for the metal functionalized by a single atom on the BS monolayer surface.

metal functionalized BS sheet and fully relaxed the structure. We have observed that a consistent change occurs in binding energy. Now, hydrogenation is done with $12H_2$ molecules, and when it had saturated, the value of the adsorption energy reached 0.106 eV for Li, 0.100 eV for Na, and 0.097 eV for K atoms [Fig. 11(a)]. After this, if we add more than $12H_2$ molecules, the adsorption energy becomes much smaller from the ideal range of 0.2 eV/H_2–0.1 eV/H_2[7]. The storage capacity of hydrogen storage can be increased by both sides of the functionalization of alkali metal adsorption and further hydrogenation. Figures 8–10 display the hydrogenation/dehydrogenation of all structures studied.

We have also calculated the desorption temperature (T_D) for all hydrogenated systems by using the von't Hoff equation as

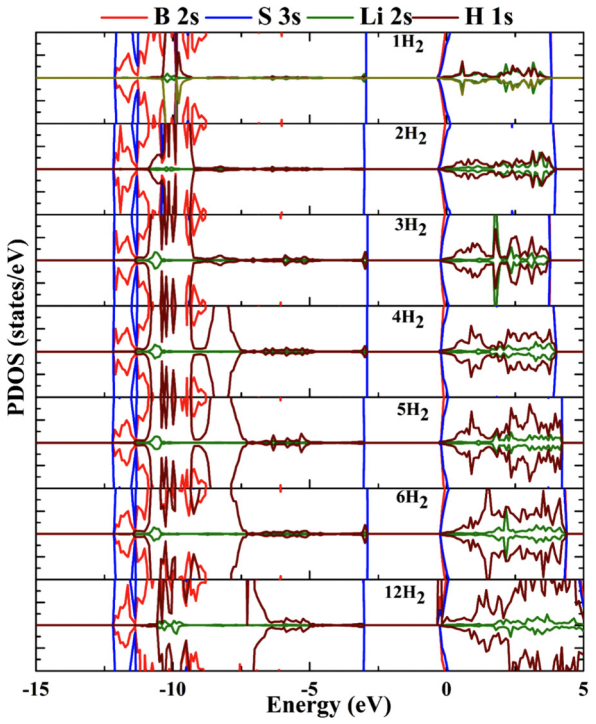

FIG. 12. Spin-polarized density of states for $1H_2$, $2H_2$, $3H_2$, $4H_2$, $5H_2$, $6H_2$, and $12H_2$ molecules adsorbed on the Li functionalized BS monolayer.

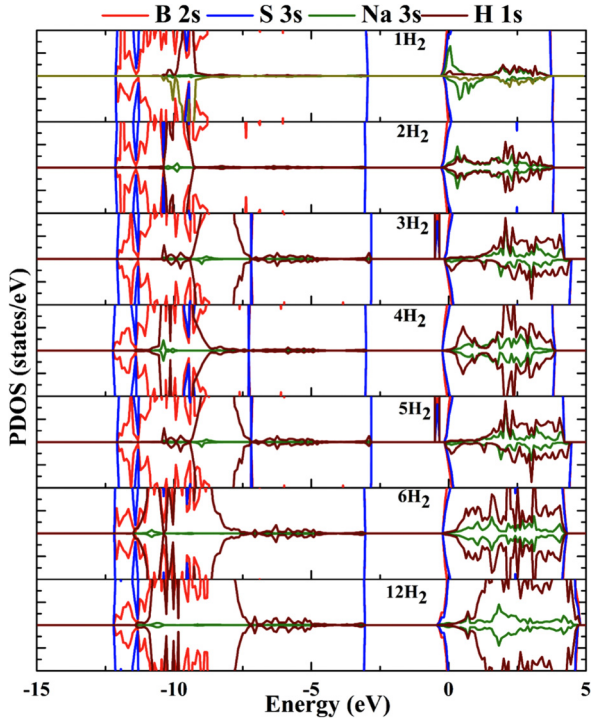

FIG. 13. Spin-polarized density of states for $1H_2$, $2H_2$, $3H_2$, $4H_2$, $5H_2$, $6H_2$, and $12H_2$ molecules adsorbed on the Na functionalized BS monolayer.

follows:[39]

$$T_D = \frac{E_{ads}}{k_b}\left(\frac{\Delta S}{R} - \ln p\right)^{-1}, \quad (5)$$

where K_{ads} is the calculated adsorption energy (in Joules per H_2 molecule), k_b is the Boltzmann constant, and the change in H_2 entropy from the gas to liquid phase is ΔS (75.44 J mol^{-1} K^{-1}). R is the universal gas constant (8.314 J mol^{-1} K^{-1}), and p is the equilibrium pressure, which is 1 atm. The values of T_D for all systems are given in Table S1 in the supplementary material and also in Fig. 11(b).

Furthermore, we performed the Bader charge analysis for all considered systems by using the formula $\Delta Q = Q_a - Q_b$ where Q_a and Q_b are the Bader charges of hydrogen molecules before and after adsorption, respectively. We observed a considerable amount of charge transfer from the alkali metal functionalized BS to hydrogen molecules as given in Table S1 in the supplementary material.

Besides, we computed spin-dependent partial density of states to examine how the orbitals of the BS sheet atoms are attached to the 1s orbital of the hydrogen molecules and alkali metals. We sketched the PDOS plot for all alkali metal (Li, Na, and K) functionalized BS sheets as shown in Figs. 12–14. From Fig. 12, in the conduction band near the Fermi level, when the number of hydrogen molecules is less, the 1s sates of hydrogen strongly hybridized with the 2s state of the Li atom, as the number of hydrogen molecules increases the number of states/eV of hydrogen increases and hybridization moves toward higher energy and becomes weaker, which is verified by the decreasing order of adsorption energy, as shown in Table S1 in the supplementary material. In the valance band, a gap is observed from 0 eV to nearly 3.0 eV. A peak of the 3s state of the S atom appears just before this bandgap. In the case of Na, from Fig. 13, we can see a similar trend, and in the case of $3H_2$ and $5H_2$ adsorption, a peak of the hybridized state of the 2p state of B and the 3p state of S is observed.

In the case of the potassium (K) functionalized BS sheet, shown in Fig. 14, for $12H_2$ in the conduction band, the asymmetric polarization of up and down states of the s-state of H_2 is obtained and in all other cases, the trend is same as that of the Li and Na functionalized BS sheet. The outcome from these graphs reveals that, when the number of hydrogen molecules is less, the 1s state of the hydrogen molecules is strongly hybridized with alkali metals, 2s, 3s, and 4s states, near the Fermi level. As the number of hydrogen molecules increases, the number of states per eV also increases and now the hybridized states move away from the Fermi level. In the valance band near the Fermi level, a gap is observed from nearly −2.5 eV to 0 eV in all PDOS graphs.

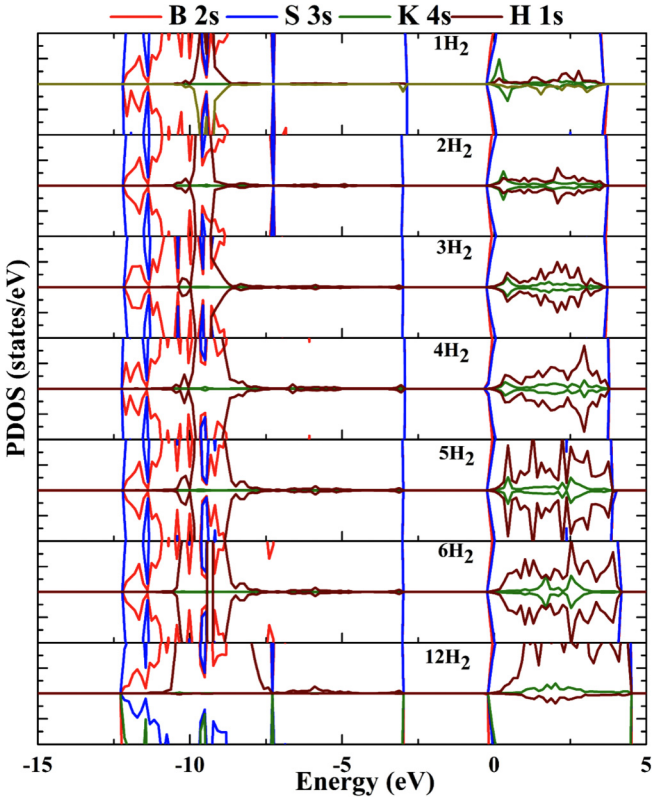

FIG. 14. Spin-polarized density of states for $1H_2$, $2H_2$, $3H_2$, $4H_2$, $5H_2$, $6H_2$, and $12H_2$ molecules adsorbed on the K functionalized BS monolayer.

V. CONCLUSIONS

We have systematically investigated the structural, electronic, vibrational, and H_2 storage properties of a BS material using spin-polarized density functional theory. Our DFT study with van der Waals correction suggests that the pristine BS monolayer has a weak binding with H_2 molecules but the binding energy can be significantly improved by alkali metal functionalization. A system energy study indicates the strong bonding of the alkali metals and the BS monolayer. The Bader charge analysis also concludes that a considerable charge is transferred from the metals to the BS sheet, which was further confirmed by charge density difference plots. All alkali metals form cations that can bond multiple hydrogen molecules with binging energies, which are excellent for H_2 storage applications. The ideal range of adsorption energy and practicable desorption temperature promises the ability of the alkali metals to functionalize the BS monolayer as an efficient material for hydrogen storage.

SUPPLEMENTARY MATERIAL

See the supplementary material for adsorption energies, desorption temperature, and the corresponding Bader charge analysis for nH_2 molecule absorption on the functionalized BS monolayer.

ACKNOWLEDGMENTS

P.M. acknowledges SVNIT, Surat, for his institute research fellowship (No. FIR-DS17PH004). D.S. and R.A. acknowledge Olle Engkvists stiftelse, Carl Tryggers Stiftelse for Vetenskaplig Forskning (CTS), and Swedish Research Council (VR) for financial support. SNIC and HPC2N are acknowledged for providing

computing facilities. Y.S. acknowledges the Science and Engineering Research Board (SERB), India, for financial support (Grant No. EEQ/2016/000217). Computational facilities from the Center for Development of Advanced Computing (C-DAC) Pune are also gratefully acknowledged.

DATA AVAILABILITY

The data that support the findings of this study are available within the article and its supplementary material.

REFERENCES

[1]D. J. Durbin and C. Malardier-Jugroot, Int. J. Hydrogen Energy **38**, 14595 (2013).
[2]C. B. Dutta and D. K. Das, Renew. Sustain. Energy Rev. **66**, 825 (2016).
[3]N. A. A. Rusman and M. Dahari, Int. J. Hydrogen Energy **41**, 12108 (2016).
[4]S. Dutta, J. Ind. Eng. Chem. **20**, 1148 (2014).
[5]P. Chen, Science **285**, 91 (1999).
[6]P. Mishra, D. Singh, Y. Sonvane, and R. Ahuja, Int. J. Hydrogen Energy **45**, 12384 (2020).
[7]J. Zhou, Q. Wang, Q. Sun, P. Jena, and X. S. Chen, Proc. Natl. Acad. Sci. U.S.A. **107**, 2801 (2010).
[8]F. E. Harris and H. S. Taylor, Physica **30**, 105 (1964).
[9]A. J. Mannix, Z. Zhang, N. P. Guisinger, B. I. Yakobson, and M. C. Hersam, Nat. Nanotechnol. **13**, 444 (2018).
[10]C. Zhai, J. Hu, M. Sun, and M. Zhu, Appl. Surf. Sci. **430**, 578 (2018).
[11]P. Srepusharawoot, E. Swatsitang, V. Amornkitbamrung, U. Pinsook, and R. Ahuja, Int. J. Hydrogen Energy **38**, 14276 (2013).
[12]T. Hussain, A. De Sarkar, and R. Ahuja, Int. J. Hydrogen Energy **39**, 2560 (2014).
[13]P. Banerjee, B. Pathak, R. Ahuja, and G. P. Das, Int. J. Hydrogen Energy **41**, 14437 (2016).
[14]P. Panigrahi, A. Kumar, A. Karton, R. Ahuja, and T. Hussain, Int. J. Hydrogen Energy **45**, 3035 (2020).
[15]Y. Ye, C. C. Ahn, C. Witham, B. Fultz, J. Liu, A. G. Rinzler, D. Colbert, K. A. Smith, and R. E. Smalley, Appl. Phys. Lett. **74**, 2307 (1999).
[16]S. Satyapal, J. Petrovic, C. Read, G. Thomas, and G. Ordaz, Catal. Today **120**, 246 (2007).
[17]D. Singh, S. K. Gupta, Y. Sonvane, and R. Ahuja, Int. J. Hydrogen Energy **42**, 22942 (2017).
[18]W. Lei, H. Zhang, Y. Wu, B. Zhang, D. Liu, S. Qin, Z. Liu, L. Liu, Y. Ma, and Y. Chen, Nano Energy **6**, 219 (2014).
[19]S. Haldar, S. Mukherjee, and C. V. Singh, RSC Adv. **8**, 20748 (2018).
[20]L. F. Chanchetti, D. R. Leiva, L. I. Lopes de Faria, and T. T. Ishikawa, Int. J. Hydrogen Energy **45**, 5356 (2020).
[21]K. Alhameedi, A. Karton, D. Jayatilaka, and T. Hussain, Appl. Surf. Sci. **471**, 887 (2019).
[22]N. S. Venkataramanan, M. Khazaei, R. Sahara, H. Mizuseki, and Y. Kawazoe, Chem. Phys. **359**, 173 (2009).
[23]S. Ould Amrouche, D. Rekioua, T. Rekioua, and S. Bacha, Int. J. Hydrogen Energy **41**, 20914 (2016).
[24]S. Grigoriev, V. Porembsky, and V. Fateev, Int. J. Hydrogen Energy **31**, 171 (2006).
[25]M. Schalenbach, M. Carmo, D. L. Fritz, J. Mergel, and D. Stolten, Int. J. Hydrogen Energy **38**, 14921 (2013).
[26]J. Niu, B. K. Rao, and P. Jena, Phys. Rev. Lett. **68**, 2277 (1992).
[27]G. J. Kubas, Acc. Chem. Res. **21**, 120 (1988).
[28]B. Mortazavi and T. Rabczuk, Energies **11**, 1573 (2018).
[29]F. Liu, P. Ming, and J. Li, Phys. Rev. B **76**, 064120 (2007).
[30]Q. Peng, W. Ji, and S. De, Comput. Mater. Sci. **56**, 11 (2012).
[31]G. Kresse and J. Furthmüller, Phys. Rev. B **54**, 11169 (1996).
[32]G. Kresse and J. Hafner, Phys. Rev. B **55**, 7539 (1997).
[33]P. E. Blöchl, Phys. Rev. B **50**, 17953 (1994).
[34]J. P. Perdew, K. Burke, and M. Ernzerhof, Phys. Rev. Lett. **77**, 3865 (1996).
[35]S. Grimme, Wiley Interdiscip. Rev. Comput. Mol. Sci. **1**, 211 (2011).
[36]H. J. Monkhorst and J. D. Pack, Phys. Rev. B **13**, 5188 (1976).
[37]P. Mishra, D. Singh, Y. Sonvane, and R. Ahuja, Sustain. Energy Fuels **4**, 2363 (2020).
[38]T. Hussain, M. Hankel, and D. J. Searles, J. Phys. Chem. C **121**, 14393 (2017).
[39]E. Durgun, S. Ciraci, and T. Yildirim, Phys. Rev. B **77**, 085405 (2008).